J. Coat. Technol. Res., **15** (5) 993–1002, 2018
https://doi.org/10.1007/s11998-017-0030-7

Structure and surface properties of a novel bulk-matte waterborne polyurethane coating composite

Qiwen Yong, Bing Liao, Guo Ying, Liang Caizhen, Hao Huang, Hao Pang

Abstract This paper reports on a novel self-matte or bulk-matte waterborne polyurethane coating composite with inherently extremely low gloss. The coating composite was comprised of a siloxane-containing waterborne polyurethane (SPU) resin and a crosslinked waterborne polyurethane (CPU) resin. The CPU resin was mainly responsible for fabricating the micro-rough surface of the film, which was achieved by a crosslinking reaction between the waterborne polyurethane and bisphenol A-type epoxy E-44 resin. The SPU resin was used to improve the comprehensive properties of the film, which was ascribed to the addition of silane coupling agent KH792. Compared with traditional matte coatings, this coating composite made it possible to avoid high loadings of matting agent and to arrive at highly flexible low-gloss finishes. Gloss levels of as low as a few tenths of a percent, even at high incidence angles, have been achieved with zero loading of extraneous dulling agent. The chemical structures of the SPU and CPU resins were characterized by FTIR-ATR and NMR spectra. The micro-rough topographies and surface rough degrees of the SPU, CPU and their 50%/50% composite films were measured by SEM and MSP, respectively. The particle sizes and particle morphologies of the SPU and CPU resins were imaged by TEM. Finally, the comprehensive properties of the SPU, CPU and their 50%/50% composite resins were evaluated, including the water contact angle, film transparency, tensile strength and storage stability.

Keywords Crosslinked waterborne polyurethane, Epoxy resin, Silane coupling agent, Bulk-matte, Low gloss, Composite film

Q. Yong, G. Ying, L. Caizhen, H. Huang, H. Pang (✉)
Key Laboratory of Cellulose and Lignocellulosics Chemistry, Guangzhou Institute of Chemistry, Chinese Academy of Sciences, Guangzhou 510650, China
e-mail: panghao@gic.ac.cn

Q. Yong, G. Ying, L. Caizhen, H. Huang
University of Chinese Academy of Sciences, Beijing 100049, China

B. Liao
Guangdong Academy of Sciences, Guangzhou 510650, China

Introduction

It is well known that the properties of waterborne polyurethanes can be easily tailored by varying the weight ratio of hard segments and soft segments, or by changing the type of hard segments and soft segments, both of which have a wide range of selectivity in material sources. Based on that, waterborne polyurethane is a highly versatile class of polymer that can be used in various fields, such as foams, elastomers, coatings, adhesives, fibers and biomaterials.[1–4] In the coatings field, most waterborne polyurethane resins, however, generally have high gloss or luster, which has always been understood to be an important characteristic for many applications, such as leather finishes, automotive body topcoats and microelectronic photoresist layers.[5] Currently, there are some applications that do not require high gloss or are preferred to not be glossy.[6] In particular, low-gloss waterborne polyurethane resins are preferred for these occasions, such as wood coatings, automotive interior topcoats and building interior finishes.[7,8] The coatings are desired to provide the low-gloss effect with a delicate texture and pleasant tactile impression on its surfaces.

From the field of optics, gloss is an optical property which indicates how well a surface reflects light in a specular direction.[9,10] The most well-known type of gloss, which gives the perception of a ''shiny'' surface,

is specular gloss.[11] Other types of gloss include surface-uniformity gloss, distinctness-of-image gloss, and contrast gloss. This article only deals with the specular gloss, which is shortened to ''gloss'' in the following text. Specular gloss depends on the amount of specular reflection in comparison to diffuse reflection.[12] The factors that affect specular gloss are the refractive index of the materials, the angle of incident light and the surface topography.[13] In the case of waterborne polyurethane resin, the variation of the refractive index is very narrow, which exerts a limited impact on the gloss. The change of the incident light angle is dependent on the external condition, which has nothing to do with the property of the resin itself. Therefore, the standard gloss reduction method for different kinds of coatings relies heavily on the control of the surface topography. The achievement of fabricating a rough topography is capable of scattering the incident light in several directions. This kind of strong light scattering ability conforms to the principle of film matting. Over the past decade, a simple approach to create rough topography relied on the addition of high concentration of large particle fillers or specially made matting agents into coatings.[4,14–17] For example, various silica particles modified with different types of waxes were the most commonly used matting agent to reduce the gloss of coatings.[18] Also, the blending of polymeric resins has been used to produce a low-gloss effect of the film, including post-blending of two fully formulated powder coatings and pre-extrusion blending of the polymeric resins into a singular coating formulation.[19–21] More complicated techniques have also been pursued by some researchers. Bauer et al.[22] utilized a dual UV lamp set-up (consisting of a 172-nm excimer lamp and a mercury arc lamp) to irradiate the acrylate formulation to create a micro-texture topography, leading to a low-gloss or matte effect of the film. Recently, a new simple method was proposed to prepare self-matte or bulk-matte aqueous coatings by fabricating large granular emulsion particles which were derived from the resin itself during the emulsion polymerization process.[23,24] These large granular emulsion particles were able to be deposited on the film surface in the film formation process. As a result, a micro-rough topography of the film was formed, producing a low-gloss or matte appearance.

In this work, we report on a novel bulk-matte waterborne polyurethane coating composition, which consists of a crosslinked waterborne polyurethane (CPU) resin and a siloxane-containing waterborne polyurethane (SPU) resin. The CPU resin was simultaneously modified by castor oil and bisphenol A-type epoxy E-44 resin, which was mainly responsible for producing the micro-rough morphology of the composite film. Meanwhile, the SPU resin was simultaneously modified with castor oil and the silane coupling agent KH792, which was designed to improve the comprehensive physical properties of the composite film, such as film transparency, film elasticity, adhesion strength and storage stability. The chemical structures of the SPU and CPU films were jointly characterized by ATR-FTIR and NMR analysis. The surface topographies and surface rough degrees of the SPU, CPU and their 50%/50% composite films were obtained by SEM and MSP, respectively. The latex particle sizes and morphologies of the SPU and CPU resins were measured by TEM observations. Finally, various physical properties of the SPU, CPU and their 50%/50% composite resins were evaluated, including film transparency, water contact angle, tensile strength and storage stability.

Experimental

Materials

Obtained were Polypropylene glycol (PPG; M_n = 2000; Guangzhou Hengyu Chemicals), castor oil (hydroxyl value = 175–185 mg KOH g-1; Sinopharm Chemical Reagent), and bisphenol A-type epoxy E-44 resin (epoxy value 0.44; Star Chemical New Material). Isophorone diisocyanate (IPDI), dimethylol butanoic acid (DMBA), dimethylol propionic acid (DMPA), triethyl amine (TEA), ethylene diamine (EDA), dibutyltin dilaurate (DBTDL) and N-(2-aminoethyl-3-aminopropyl)trimethoxysilane (KH792) were purchased from Shanghai Aladdin Reagent.

Preparation of the siloxane-containing waterborne polyurethane (SPU) resin

Synthesis of the SPU resin was carried out in a 500-mL round-bottom flask equipped with a mechanical stirrer, a thermometer and a condenser with a drying tube. IPDI, PPG ($R_{NCO/OH}$ = 4) and castor oil (8.5% of the prepolymer weight) in the presence of catalyst DBTDL were added to the flask and maintained at 70°C for 2 h at a constant stirring speed of 250 rpm. Subsequently, DMBA (6.5% of the prepolymer weight) diluted with acetone solvent was added into the flask and heated at 75°C for 3 h. The reactor was cooled to 45°C, and TEA was added and stirred for 30 min to neutralize the carboxylic acid moieties. Finally, the KH792 (2% of the prepolymer weight) and a certain amount of water was added under the vigorous stirring rate for 1 h to obtain the SPU resin.

Synthesis of the crosslinked waterborne polyurethane (CPU) resin

First, PPG and castor oil (3% of the prepolymer weight) were added to a vessel and stirred for 30 min to obtain a homogeneous mixture. Prepolymerization was carried out at 75°C for 2 h by adding IPDI ($R_{NCO/OH}$ = 4) under nitrogen atmosphere in the presence of DBTDL as the catalyst. Then, DMPA (7.5% of the

prepolymer weight) and bisphenol A-type epoxy E-44 resin (7% of the prepolymer weight) diluted with acetone solvent were added to the reactor for 3 h. The reactor was cooled to 40°C, and TEA was added to neutralize the carboxylic groups of DMPA for 30 min. During the dispersive process, the resultant prepolymer was dropwise added into a new vessel which was filled with EDA and a great amount of deionized water. The reaction was maintained for 1 h to obtain the CPU resin.

Preparation of the individual SPU, CPU and composite films

The individual SPU, CPU and their composite resins with different weight ratios ranging from 10% SPU/90% CPU to 90% SPU/10% CPU were poured onto glass molds. After being dried at room temperature for 48 h and then at 50°C in a vacuum oven for 24 h, the films were peeled from the glass molds and stored in a desiccator at ambient temperature. Then, we carried out some simple tests on the different proportions of the SPU and CPU resins, such as the hardness, adhesion strength, film flexibility, film touch-feeling and film appearance, etc. The 50% SPU/50% CPU composite film had an excellent balance between the hardness, adhesion strength and film flexibility. Accordingly, all the following characterizations were based on the individual SPU, CPU and their 50% SPU/50% CPU composite resins.

Characterization

Attenuated total reflection-Fourier transform infrared spectroscopy (ATR-FTIR). The infrared spectra of the individual SPU and CPU films were obtained on a Bruker VERTEX70 FTIR spectrometer under N_2 purging. Each sample was scanned 16 times at a resolution of 1 cm^{-1} over the frequency range of 4000–600 cm^{-1}.

Nuclear magnetic resonance (NMR). ^{1}HNMR and ^{13}CNMR spectra of the individual SPU and CPU films were recorded on a Bruker DRX-400 spectrometer. The solvent was $CDCl_3$. Tetramethylsilane was used for the internal reference.

Scanning electron microscopy (SEM). The micro-rough topographies of the individual SPU, CPU and their 50% SPU/50% CPU composite films were observed using a Zeiss-Merlin SEM. The dried films were stained on a copper grid. Then, the gold was sprayed on the films to enhance the conductivity.

Mechanical surface profilometer (MSP). The rough surfaces of the individual SPU, CPU and their 50%/50% composite films were scanned in straight lines ''1D'' with a stylus-based mechanical profilometer (Tencor P-10 surface profiler; KLA-Tencor, CA, USA). A stylus contact force of 1 mg was used.

Transmission electron microscopy (TEM). The particle sizes and particle morphologies of the individual SPU and CPU resins were observed by TEM (JEM-2100F) with a 100-kV electron beam. Both resins were diluted to 500 ppm with deionized water containing 2% phosphotungstic acid. Micro-copper grids were dipped into them for a while and taken out for drying at ambient temperature overnight.

Ultraviolet visible spectroscopy (UV–Vis). The transmittances of the films were measured by a single-beam UV-2550 spectrophotometer. The air was used for calibration. Then, the films were stuck on the sample cell for analysis. The measured wavelength ranged from 200 nm to 800 nm with a medium speed of scanning.

Tensile test Mechanical properties of the SPU, CPU and their 50% SPU/50% CPU composite films were assessed by tensile tests. Small bone-shaped specimens were cut from the free films.[25,26] The specimens had an overall length of 80 mm and widths of 6 mm and 25 mm in the stretching and clamping zone, respectively. Film thickness ranged between 100 and 200 μm. The tensile tests were performed by a universal testing machine (Shenzhen Reger Instrument, China). A crosshead speed of 50 mm min^{-1} was used to determine the ultimate tensile strengths and elongations at break (%) for all the specimens. The resultant values were reported as the average of five measurements.

Water contact angle (WCA). DSA 10 video contact angle measuring equipment was used to measure the water contact angles of the individual SPU, CPU and their 50%/50% composite films. Three independent measurements were made on different parts of the films. The average water contact angle values were reported.

Physical properties. The specular glosses of the films were determined at 60° incident angle using a KGZ-60 gloss meter according to ASTM E 284. The gloss values were measured five times for each sample. The hardness of the films was determined using an SDI-TH200 Shore A type durometer. The adhesion strengths of the films were tested with commercial Sellotape using the cross-cut adhesion test method (ASTM D3359). The test results were presented using a rating of 0B for a low adherent coating through 5B for a high adherent coating. The stored stabilities of the resins were also evaluated.

Results and discussion

Chemical structural characterization

In Fig. 1, the ATR-FTIR spectra have been used to identify the characteristic chemical structures of the SPU and CPU films. In both samples, the peaks at 3347 cm^{-1} [v(–NHCOO–)], 2870–2974 cm^{-1} [v(–CH_2–) and v(–CH_3)], 1703 cm^{-1} [v(–C=O)], 1556 cm^{-1} [δ(–NHCOO–)] and 1103 cm^{-1} [v(–C–O–C-)] belonged

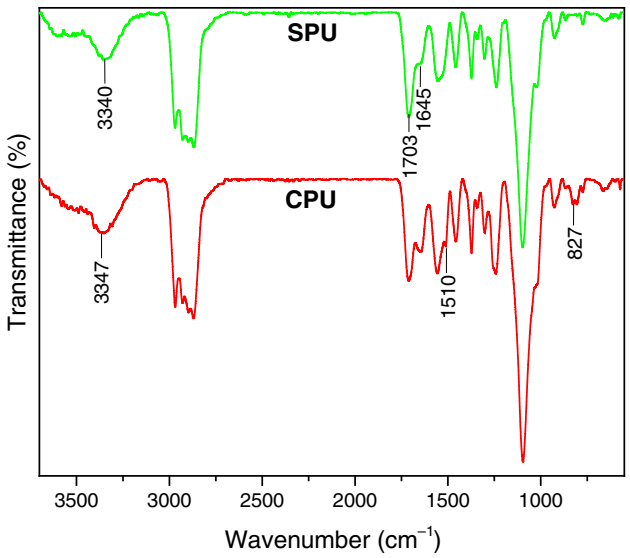

Fig. 1: ATR-FTIR spectra of the SPU and CPU films

to the typical polyurethane structure, while the peak at 1645 cm^{-1} was ascribed to the unsaturated C=C bonds of the castor oil. In the SPU spectrum, an absence of the characteristic band at 3288 cm^{-1} [v (–NH_2) and v (–NH–)] indicated that the amino groups of the KH792 had reacted with the isocyanate-terminated polymers. These results showed that the waterborne polyurethane simultaneously modified with the castor oil and KH792 was successfully prepared. In the CPU spectrum, the peaks at 1510 and 827 cm^{-1} were ascribed to the C=C skeleton vibrations and =C–H out-of-plane bending vibrations of the epoxy E-44 resin, respectively. Furthermore, the characteristic peak of the epoxy groups at 910 cm^{-1} disappeared, demonstrating that the ring-opening reaction of the epoxy groups occurred. In conclusion, the crosslinked waterborne polyurethane simultaneously modified with the castor oil and bisphenol A-type epoxy E-44 resin was successfully synthesized.

Figure 2 shows the ^{1}HNMR and ^{13}CNMR spectra of the SPU and CPU films. In the SPU-^{1}HNMR spectrum, the strong peak at 7.26 ppm was assigned to the $CDCl_3$ solvent. The two symmetrical peaks at 7.00 and 7.52 ppm were attributed to the urethane groups, which were fabricated by the chemical reaction between the two isocyanate groups of the IPDI and hydroxyl groups. The peak at 6.92 ppm was ascribed to the urea groups, which were caused by the reaction between the isocyanate groups and amino groups of the KH792. The peaks at 5.19, 5.29 and 5.39 ppm were ascribed to the –C=C–H of the castor oil. In the SPU-^{13}CNMR spectrum, the resonance at 206.40 ppm was the solvent peak of acetone. The resonance at 179.35 ppm was ascribed to the –COOH of the DMBA, and the resonance at 172.77 ppm was attributed to the –COOR of the castor oil. The peaks at 157.29 and 155.06 ppm corresponded to all kinds of urea and urethane groups. The peaks at 121.41, 124.12 and 131.86 ppm were attributed to the unsaturated C=C bonds of the castor oil. The combined characterization of the ATR-FTIR and NMR spectra demonstrates that the siloxane-containing waterborne polyurethane resin modified by the KH792 and castor oil was successfully fabricated. In the CPU-^{1}HNMR spectrum, it is obvious that two peaks at 7.52 and 7.00 ppm had the same peak intensity. These two resonances correspond to the two kinds of –NHCOO– groups, respectively, when two isocyanate groups of the IPDI reacted with hydroxyl groups. Similarly, the four symmetrical peaks at 7.14, 7.12, 6.82, 6.80 ppm were attributed to the hydrogen protons on the benzene ring skeletons of the bisphenol A-type epoxy E-44 resin. The strongest peak at 7.26 ppm was the $CDCl_3$ solvent. The emergence of the weak peak at 5.07 ppm possibly resulted from the unsaturated –C=C–H of the castor oil. However, in the CPU-^{13}CNMR spectrum, the peak at 206.01 ppm was caused by the remaining solvent acetone. The small resonance at 178.12 ppm was ascribed to the carboxyl groups of the DMPA. The band ranging at 154.86–156.73 ppm was attributed to all kinds of –NHCOO– groups. The symmetrical peaks of the two groups (113.42 and 127.12 ppm, 142.92 and 155.74 ppm) were attributed to the carbon resonances of the benzene ring skeleton of the epoxy E-44 resin. Apart from that, the peaks at 121.25, 124.06 and 124.21 ppm (–C=C–) and the peak at 8.39 ppm (–CH_3) were certainly from the castor oil. Combined with the ATR-FTIR spectra, all these results indicate that the CPU resin simultaneously modified by the bisphenol A-type epoxy E-44 resin and castor oil was successfully prepared.

Particle morphology observation

Figure 3 shows the TEM images of the SPU and CPU latex particles. It can be seen that nearly all the SPU latex particles were spherical in shape. They were well dispersed and exhibited no sticky behavior with each other, and they embraced uniform sizes with a diameter of 30 ± 5 nm around the mean value. However, the CPU latex particles exhibited an irregular spherical shape with a diameter about 25 ± 5 nm, which was slightly smaller than that of the SPU particles. Also, compared with the mono-dispersed SPU latex particles, the CPU particles exhibited a certain sticky behavior, which was easy to agglomerate between many particles. This is due to the fact that the introduction of the bisphenol A-type epoxy E-44 resin caused the latex system to be unstable to some extent. Thus, it is wise to compound to be the SPU and CPU resins to improve the latex storage stability.

Film surface analysis

As can be seen from Fig. 4, the SEM images show the surface morphologies of the SPU, CPU and their 50%/

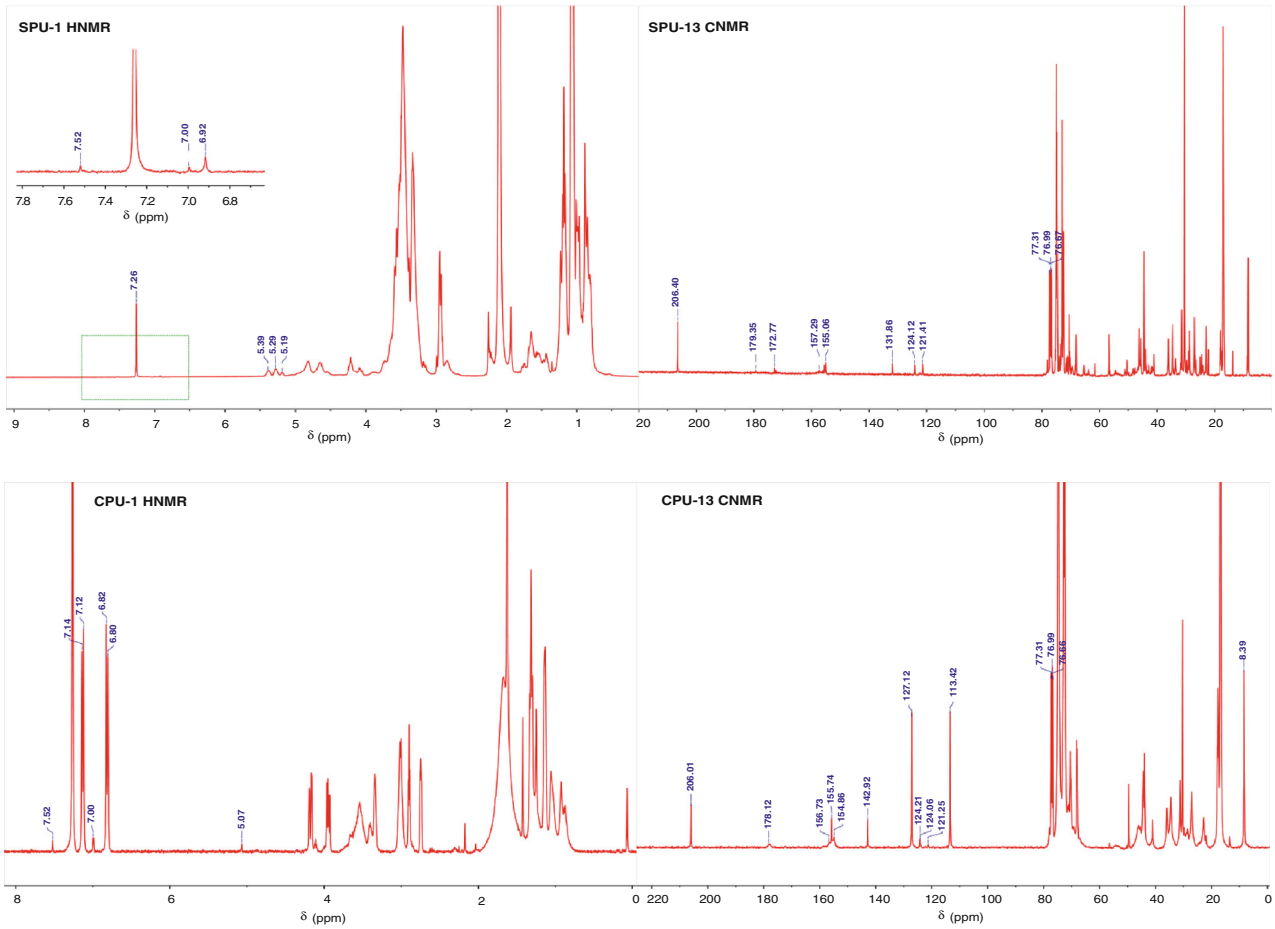

Fig. 2: ^{1}HNMR and ^{13}CNMR spectra of the SPU and CPU films

50% composite films. The Surface Profilometer measurement shows the line scanning curves of film surfaces in order to obtain the surface roughness parameters. In general, characterizing surface roughness involves a consideration not only of the spread of heights about a reference plane (the root mean square roughness R_q) but also the variation of heights over the surface (the average surface wavelength λ_a).[27] It is apparent that the surface morphology of the SPU film was quite flat and smooth; the R_q and λ_a values were 0.45 and 69 μm, respectively. In contrast, the CPU film surface was coarse and uneven and the R_q and λ_a values were 1.92 and 42 μm, respectively. This is due to the special flow behavior of an elastoviscous liquid which can lead to a rough surface. This process can occur whether shrinkage takes place or not, until a point is reached where resistance to flow exceeds the available shear stress due to surface tension. The generation of a micro-rough surface of the appropriate dimensions is related to the early development of elastic forces during film formation.[28] Therefore, the CPU resin was highly crosslinked in molecular structure, and the early-staged elastic forces of the CPU resin were far greater than that of the SPU films, thus forming a significantly micro-rough surface after film formation. It is universally acknowledged that the surface gloss of a film is significantly dependent on the surface roughness.[29,30] In some cases, the rougher the film surface, the lower the specular gloss.[31,32] Thus, the specular gloss of the SPU film was much greater than that of the CPU film. However, if the surface is rough on the order of several millimeters, the gloss could still be quite high and the roughness could be quite high, which is due to the λ_a value being too large and so unable to effectively scatter the incident light on its surface. In conclusion, the gloss of a material depends on the surface roughness near the wavelength of the illuminating light. The film surface of the 50%/50% composite was also rough, and the R_q and λ_a values were 1.28 and 59 μm, respectively, which was between that of the individual SPU film and the individual CPU film. Even though the gloss degree of the composite film was a little greater than that of the individual CPU film, the composite film was able to afford good transparency, good storage stability, good tensile property and excellent adhesive strength compared with the individual CPU film.

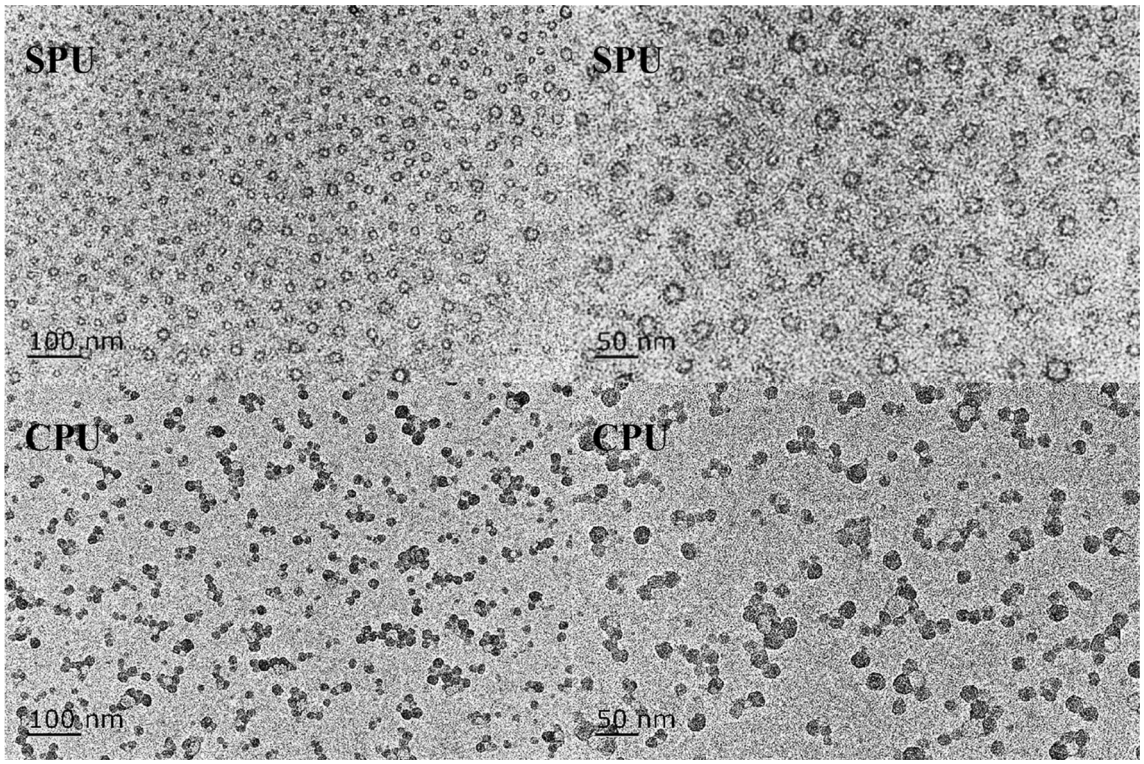

Fig. 3: TEM images of the SPU and CPU latex particles

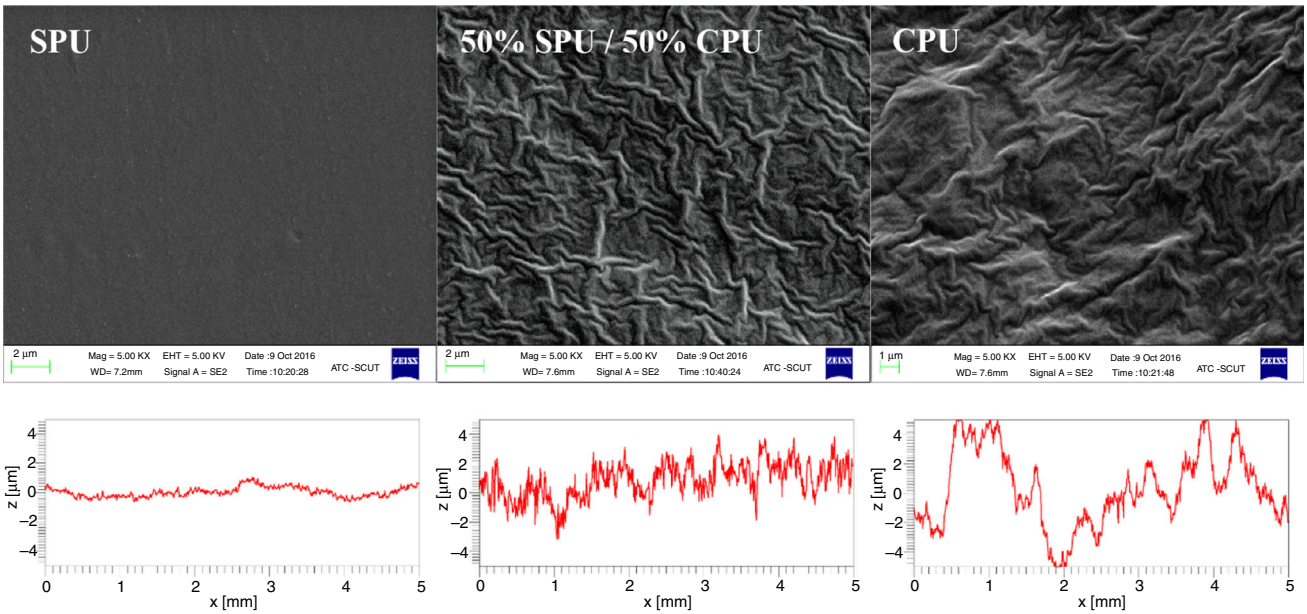

Fig. 4: SEM images and line scanning curves of the SPU, CPU and their 50%/50% composite films

Film transparency

Film transparency is a significant property of films, since it has a direct impact on the appearance of the coated product.[33] In Fig. 5, the film transparencies of SPU, CPU and their 50%/50% composite films were measured by UV–Vis spectra. Because the UV–Vis equipment was a single-beam spectrophotometer, we measured all the light transmitted instead of the scattered light. It is obvious that none of the three samples had absorption in the wavelengths ranging from 200–300 nm. When it came to the visible light

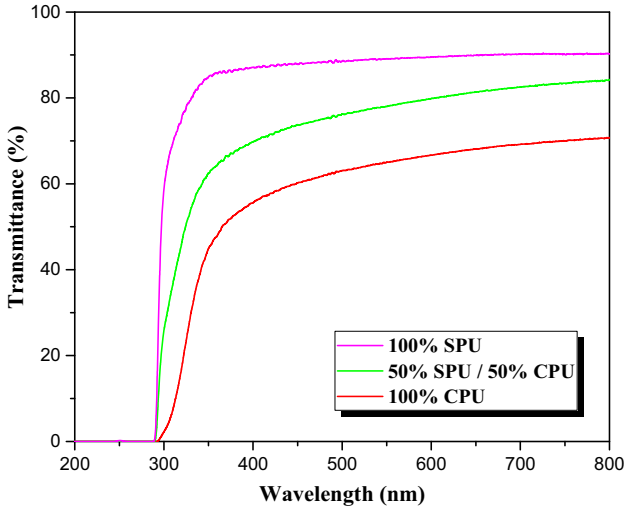

Fig. 5: Film transparency of the SPU, CPU and their 50%/50% composite films

(400–800 nm range), each sample exhibited a different degree of light absorption. The individual SPU film had the highest transmittance value up to 90%, whereas in contrast the individual CPU film embraced the lowest transmittance value of 65%. When blending the SPU and CPU resins in equal portions, the light transmittance reached about 80%. These results show that the introduction of the SPU resin into the CPU resin significantly improved the film transparency.

Film tensile property

As shown in Table 1, the individual CPU film demonstrated the highest tensile strength of 26 MPa and the lowest elongation at break of 248%. Therefore, the elastic property of the CPU film was poor. This result was mainly due to an increase in crosslinking density provided by the bisphenol A-type epoxy E-44 resin. In contrast, the individual SPU film showed the lowest tensile strength of 12 MPa with the highest elongation at break of 440%. As a result, the tensile strength of the individual SPU film was a little too low to meet the practical demand. However, when adding a certain amount of the SPU into CPU, such as 50% of total weight, the elongation at break of the composite film increased to 335% and the tensile strength was approximately 20 MPa, endowing the composite film with good elasticity.

Water contact angle

It is worth noting that the actual solid film has a certain roughness. Dependence on the wetting characteristics of a solid film on the roughness of its surface is inherent.[34,35] Figure 6a presents an ideal smooth surface of a solid film. Whenever a process involves the

Table 1: Tensile property of the SPU, CPU and their 50%/50% composite films

Sample	Tensile strength (MPa)	Elongation at break (%)
100% SPU	12	440
50% SPU/50% CPU	20	335
100% CPU	26	248

wetting of a solid film by a liquid, three different interfacial boundary surfaces, i.e., solid–liquid, solid–air, and liquid–air, are involved. The wetting process involves replacing an area of the solid–air interface (δ_s) with an equal area of the solid–liquid interface (δ_s), and meanwhile involves an extension of the liquid–air interface ($\delta_s \cdot \cos\theta$). Assuming that the system always keeps a balance when wetting is proceeding spontaneously from the A to B points, it should be written:

$$\gamma_{SL}\delta_S + \gamma_{LV}\delta_S \cos\theta - \gamma_{SV}\delta_S = 0 \tag{1}$$

$$\cos\theta = \frac{\gamma_{SV-}\gamma_{SL}}{\gamma_{LV}} \tag{2}$$

Figure 6b reveals the wetting behavior of a rough surface film, assuming that the wetting angle of the rough film is θ_n. The wetting process also involves replacing an area of the solid–air interface ($n \cdot \delta_s$) with an equal area of the solid–liquid interface ($n \cdot \delta_s$). However, the surface area of the liquid–air interface still stays at $\delta_s \cdot \cos\theta_n$. The wetting process on a rough surface film could be expressed by:

$$\gamma_{SL} \cdot n\delta_S + \gamma_{LV}\delta_S \cos\theta_n - \gamma_{SV} \cdot n\delta_S = 0 \tag{3}$$

Combined with equations (2) and (3), this shows that:

$$\cos\theta_n = \frac{n(\gamma_{SV-}\gamma_{SL})}{\gamma_{LV}} = n\cos\theta. \tag{4}$$

$$\frac{\cos\theta_n}{\cos\theta} = n \tag{5}$$

where n is defined as the coefficient of surface roughness. The actual surface area of a rough solid film must be greater than an ideal smooth surface with the same geometric shape and dimension, so $n > 1$, $\cos\theta_n > \cos\theta$. If $\theta < 90°$, $\theta_n < \theta$; $\theta = 90°$, $\theta n = \theta$; $\theta_n > 90°$, $\theta n > \theta$. Therefore, it demonstrates that, if $\theta < 90°$, the contact angle decreases with the increase of surface roughness and if $\theta > 90°$, the contact angle increases with increasing the surface roughness.

In Fig. 7, there is a strong indication that the surface roughness has a great influence on the wetting behavior. Due to the film surface of SPU being very smooth, the root mean square roughness, R_q, was only 0.45 μm and the water contact angle was about 98°. However,

the individual CPU film surface was quite rough and uneven, so R_q was up to 1.92 μm, and the value of the water contact angle was approximately 119°. These results indicate that, when the wetting angle of the film was greater than 90°, the water contact angle increased with the increase of the surface roughness, which was in accordance with the above theory. The surface of the composite film was also rough (R_q = 1.28 μm), but the degree of surface roughness was smaller than that of the individual CPU film. Thus, the water contact angle of the composite film was 110°, still offering excellent hydrophobic ability.

Physical properties

Table 2 shows the physical properties of the individual SPU, CPU and their 50%/50% composite. The Shore A hardness of the individual SPU film was 54, which was a little bit soft for applications. The Shore A hardness of the individual CPU film was up to 75. This is due to the addition of the bisphenol A-type epoxy E-44 resin, which contained many rigid phenyl skeleton structures. The composite film hardness was 65, which possessed a moderate hardness and good elasticity, endowing the film with a soft-touch feeling. In addition, the adhesive strength of the composite film increased due to the addition of the SPU resin into the CPU resin. In the case of the specular gloss at 60° incident angle, the individual SPU film embraced a very high gloss value of up to 92 units. The gloss of the individual CPU film was only 6 units. The gloss of the 50%/50% composite film increased slightly to 14 units.

As for the storage stability, the individual CPU sample easily cohered or formed into a mass after incubating for a few weeks, which was in accordance with the result of the TEM observations. The individual SPU and 50%/50% composite resins were validated over 6 months from the date of manufacture and showed an excellent storage stability. These results demonstrate that the addition of the SPU resin into the CPU resin significantly enhanced the storage stability.

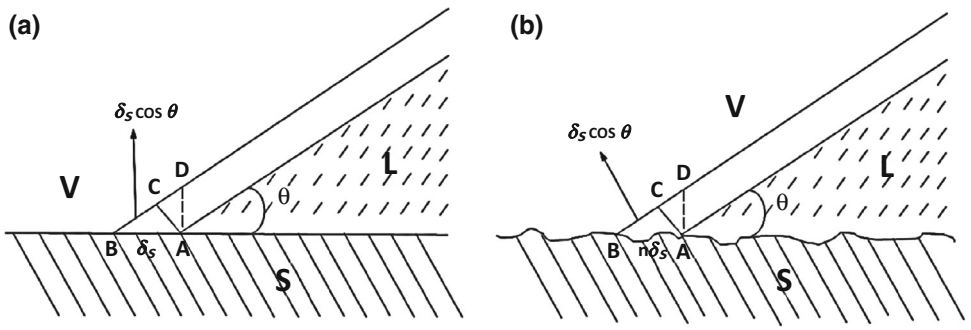

Fig. 6: Wetting behaviors of a liquid on a smooth solid film and a rough solid film, respectively

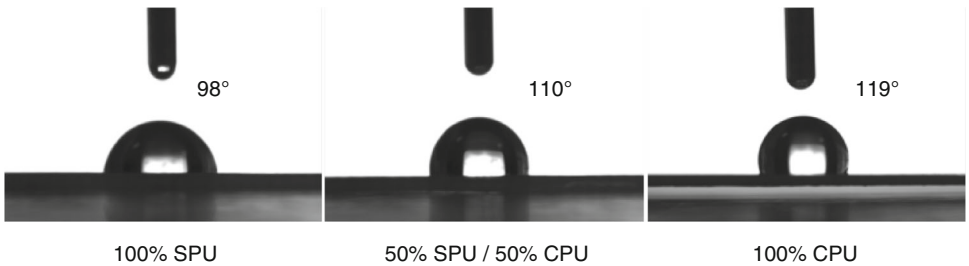

Fig. 7: Water contact angle analysis of the SPU, CPU and their 50%/50% composite films

Table 2: Physical properties of the individual SPU, CPU and their 50%/50% composite

Sample	Shore A hardness	Adhesive strength	60° gloss	Storage stability
SPU	54	5B	92	Over 6 months
50%/50% composite	65	5B	14	Over 6 months
CPU	75	4B	6	A few weeks

Conclusions

A novel bulk-matte waterborne polyurethane resin composite containing both SPU and CPU resins was successfully synthesized. The composite resin was able to form a micro-rough surface spontaneously during the film-forming process without the addition of any matting agents, leading to the bulk-matte effect of the film. The research shows that the 50% SPU and 50% CPU in weight ratio was able to provide the optimal comprehensive property of the composite film, which endowed the film with a delicate texture and soft-touch feeling. The root mean square roughness of the composite film was 1.28 μm, which made the refined surface structure difficult to see with the naked eye. The specular gloss of the composite film was 14 units, which provided the film with an excellent matting effect. Compared with the individual CPU resin, the 50%/50% composite resin was able to afford the cast film with good transparency, good tensile property, good storage stability and superior adhesive strength, making it a very good prospective alternate coating for various matte applications.

Acknowledgment This research was supported by Science and Technology Planning Project of Guangdong Province, China (Grant No. 2015A010105001).

Compliance with ethical standard

Conflict of interest The authors declare no competing financial interest.

References

1. He, Yong, Xie, Delong, Zhang, Xinya, ''The Structure, Microphase-Separated Morphology, and Property of Polyurethanes and Polyureas.'' *J. Mater. Sci.*, **49** (21) 7339–7352 (2014)
2. Polus, I, ''Synthesis of Polyurethane Coating Components with IPDI and TMDI.'' *Holz als Roh-und Werkstoff*, **61** (3) 238–240 (2003)
3. Princi, Elisabetta, et al., ''On the Micro-Phase Separation in Waterborne Polyurethanes.'' *Macromol. Chem. Phys.*, **210** (10) 879–889 (2009)
4. Zhou, Xing, et al., ''Recent Advances in Synthesis of Waterborne Polyurethane and Their Application in Water-Based Ink: A Review.'' *J. Mater. Sci. Technol.*, **31** (7) 708–722 (2015). https://doi.org/10.1016/j.jmst.2015.03.002
5. Basu, Soumendra K, Scriven, LEE, Francis, LFF, McCormick, AVV, ''Mechanism of Wrinkle Formation in Curing Coatings.'' *Prog. Org. Coat.*, **53**(1): 1–16 (2005) http://linkinghub.elsevier.com/retrieve/pii/S0300944004002103
6. Kitaike, Y, Hatakeyama, H, Tayama, S, Nakagawa, K, ''Mat Thermoplastic Resin Composition and Laminate Therefrom, Matting Agent Therefore, and Method for Matting Thermoplastic Resin.''(1996)
7. Hong, J K, et al. ''Low Gloss Thermoplastic Resin Composition with Soft Touch Surface and Molded Article Therefrom.'' (2016)
8. Shimamoto, Y, Nishimura, J, *Shimamoto, N –2007–Acrylic Matt Thermoplastic Resin Films and Process for Producing the Same.pdf*. US (2007).
9. Vessot, K, Messier, P, Hyde, J M, Brown, C A, ''Correlation between Gloss Reflectance and Surface Texture in Photographic Paper.'' *Scanning*, **37**(3): 204–17 (2015) http://doi.wiley.com/10.1002/sca.21201.
10. Villalobos, R, et al., ''Gloss and Transparency of Hydroxypropyl Methylcellulose Films Containing Surfactants as Affected by Their Microstructure.'' *Food Hydrocoll.*, **19**(1): 53–61 (2005) http://linkinghub.elsevier.com/retrieve/pii/S0268005X04000529.
11. Trezza, T A, Krochta, J M, ''Specular Reflection, Gloss, Roughness and Surface Heterogeneity of Biopolymer Coatings.'' *J. Appl. Polym. Sci.*, **79**(12): 2221–29 (2001) http://doi.wiley.com/10.1002/1097-4628%2820010321%2979%3A12%3C2221%3A%3AAID-APP1029%3E3.0.CO%3B2-F.
12. Chadwick, A C, Kentridge, R W, ''The Perception of Gloss: A Review.'' *Vis. Res.*, **109**(PB) 221–35 (2015) https://doi.org/10.1016/j.visres.2014.10.026.
13. Juuti, M, et al., ''Detection of Local Specular Gloss and Surface Roughness from Black Prints.'' *Coll. Surf. A: Physicochem. Eng. Asp.*, **299**(1–3): 101–8 (2007) http://linkinghub.elsevier.com/retrieve/pii/S0927775706008739.
14. Cawthorne, James Edwin, Joyce, Margaret, Fleming, Dan, ''Use of a Chemically Modified Clay as a Replacement for Silica in Matte Coated Ink-Jet Papers.'' *J. Coat. Technol.*, **75** (2) 75–81 (2003)
15. Dullaert, Konraad, Steeman, Paul, Bolks, Jurjen, ''A Mechanistic Study of the Effect of Pigment Loading on the Appearance of Powder Coatings: the Effect of Surface Topography on the Optical Properties of Powder Coatings: Modelling and Experimental Results.'' *Prog. Org. Coat.*, **70** (4) 205–212 (2011). https://doi.org/10.1016/j.porgcoat.2010.07.014
16. Lee, Sang Sun, et al., ''Gloss Reduction in Low Temperature Curable Hybrid Powder Coatings.'' *Prog. Org. Coat.*, **46** (4) 266–272 (2003)
17. Ou, Juhua, et al., ''Matting Films Prepared from Waterborne Acrylic/micro-SiO2 Blends.'' *J. Appl. Polym. Sci.*, **132** (13) 1–8 (2015)
18. Colombo, A et al. ''Highly Transparent poly(2-Ethyl-2-Oxazoline)-TiO 2 Nanocomposite Coatings for the Conservation of Matte Painted Artworks.'' *RSC Adv.*, **5**(103): 84879–88 (2015) http://xlink.rsc.org/?DOI=C5RA10895K.
19. Giles, S L, et al., ''Novel Methods of Producing Low-Reflectance Coatings Utilizing Synergistic Effects of Polymer Phase Separation.'' *ACS Appl. Mater. Interfaces*, **8**(39): 26251–57 (2016) http://pubs.acs.org/doi/abs/10.1021/acsami.6b06037.
20. Thometzek, P, Freudenberg, U, Meier-Westhues, U, Yonek, K, ''Weather-Stable Low-Gloss Powder Coatings.'' *J. Coat. Technol.*, **72**(7): 75–79 (2000) http://dx.doi.org/10.1007/BF02698473%5Cnhttp://link.springer.com/10.1007/BF02698473.
21. Xue, L, Zhang, J, Han, Y, ''Phase Separation Induced Ordered Patterns in Thin Polymer Blend Films.'' *Prog. Polym. Sci.*, **37**(4): 564–94 (2012) http://linkinghub.elsevier.com/retrieve/pii/S0079670011001067.
22. Bauer, F, et al., ''UV Curing and Matting of Acrylate Nanocomposite Coatings by 172 nm Excimer Irradiation.'' *Prog. Org. Coat.*, **64**(4): 474–81 (2009) http://linkinghub.elsevier.com/retrieve/pii/S0300944008001999.

23. Cao, Xianli, Ge, Xia, Chen, Huanhuan, Li, Wenbo, ''Effects of Trimethylol Propane and AAS Salt on Properties of Waterborne Polyurethane with Low Gloss.'' *Prog. Org. Coat.*, **107** 5–13 (2017). https://doi.org/10.1016/j.porgcoat.2017.02.021
24. Yong, Q, et al., ''Synthesis and Surface Analysis of Self-Matt Coating Based on Waterborne Polyurethane Resin and Study on the Matt Mechanism.'' *Polym. Bull.*, **74**(4): 1061–76 (2017) http://link.springer.com/10.1007/s00289-016-1763-7.
25. Rahman, MM, et al. ''Synthesis and Properties of Polyurethane Coatings: The Effect of Different Types of Soft Segments and Their Ratios.'' *Composite Interfaces*, **20**(1): 15–26 (2013) http://dx.doi.org/10.1080/15685543.2013.762890%5Cnhttp://www.tandfonline.com/doi/abs/10.1080/15685543.2013.762890.
26. Zhai, L, et al., ''Synthesis and Characterization of Nanosilica/waterborne Polyurethane End-Capped by Alkoxysilane via a Sol-Gel Process.'' *J. Appl. Polym. Sci.*, **128**(3): 1715–24 (2013) http://doi.wiley.com/10.1002/app.38225.
27. Fletcher, TE, ''A Simple Model to Describe Relationships between Gloss Behaviour, Matting Agent Concentration and the Rheology of Matted Paints and Coatings.'' *Prog. Org. Coat.*, **44** (1) 25–36 (2002)
28. Bernotti, Lorenzo, Fletcher, Tim, Ferner, Uwe, ''Making Matte Finishes to Meet New Challenges.'' *Eur. Coat. J.*, **11** 30–32 (2011)
29. Faucheu, J, Wood, K A, Sung, L P, Martin, J W, ''Relating Gloss Loss to Topographical Features of a PVDF Coating.'' *J. Coat. Technol. Res.,* **3**(1): 29–39 (2006) http://www.scopus.com/inward/record.url?eid=2-s2.0-32544445970&partnerID=tZOtx3y1.
30. Järnström, J, Ihalainen, P, Backfolk, K, Peltonen, J, ''Roughness of Pigment Coatings and Its Influence on Gloss.'' *Appl. Surf. Sci.*, **254** (18) 5741–5749 (2008)
31. Alexander-Katz, R, Barrera, R G, ''Surface Correlation Effects on Gloss.'' *J. Polym. Sci. Part B: Polym. Phys*., **36**(8) 1321–34 (1998) http://www.fisica.unam.mx/personales/rbarrera/pdf/pub/int/57-JPolymerS-B-36-1321-98.pdf%5Cnhttp://doi.wiley.com/10.1002/(SICI)1099-0488(199806)36:8%3C1321::AID-POLB7%3E3.0.CO;2-U
32. Gunde, M K, Kunaver, M, Čekada, M, ''Surface Analysis of Matt Powder Coatings.'' *Dyes Pigments*, **74**(1): 202–7 (2006) http://linkinghub.elsevier.com/retrieve/pii/S0143720806000684.
33. Maia, R, D'Alba, L, Shawkey, M D, ''What Makes a Feather Shine? A Nanostructural Basis for Glossy Black Colours in Feathers.'' *Proc. R. Soc. Lond. B*, **278**(1714): 1973–80 (2011) http://rspb.royalsocietypublishing.org/cgi/doi/10.1098/rspb.2010.1637.
34. Blumenthal, James, Barefoot, John, Haney, Tom, ''Communication to the Editor.'' *J. Psychosom. Res.*, **30** (3) 387 (1986)
35. Wenzel, R N, ''Resistance of Solid Surfaces to Wetting by Water.'' *Ind. Eng. Chem.*, **28**(8): 988–94 (1936) http://pubs.acs.org/doi/abs/10.1021/ie50320a024.